# Superradiance for Atoms Trapped along a Photonic Crystal Waveguide

A. Goban, C.-L. Hung, J. D. Hood, S.-P. Yu, J. A. Muniz, O. Painter, and H. J. Kimble

Phys. Rev. Lett. **115**, 063601 — Published 5 August 2015

DOI: 10.1103/PhysRevLett.115.063601

# Superradiance for atoms trapped along a photonic crystal waveguide

A. Goban[1,2,†], C.-L. Hung[1,2,†,‡], J. D. Hood[1,2,†], S.-P. Yu[1,2,†],
J. A. Muniz[1,2], O. Painter[2,3], and H. J. Kimble[1,2,*]
[1] *Norman Bridge Laboratory of Physics 12-33*
[2] *Institute for Quantum Information and Matter, California Institute of Technology, Pasadena, CA 91125, USA and*
[3] *Thomas J. Watson, Sr., Laboratory of Applied Physics 128-95*
(Dated: July 14, 2015)

We report observations of superradiance for atoms trapped in the near field of a photonic crystal waveguide (PCW). By fabricating the PCW with a band edge near the $D_1$ transition of atomic cesium, strong interaction is achieved between trapped atoms and guided-mode photons. Following short-pulse excitation, we record the decay of guided-mode emission and find a superradiant emission rate scaling as $\bar{\Gamma}_{\rm SR} \propto \bar{N} \cdot \Gamma_{\rm 1D}$ for average atom number $0.19 \lesssim \bar{N} \lesssim 2.6$ atoms, where $\Gamma_{\rm 1D}/\Gamma' = 1.0 \pm 0.1$ is the peak single-atom radiative decay rate into the PCW guided mode and $\Gamma'$ is the radiative decay rate into all the other channels. These advances provide new tools for investigations of photon-mediated atom-atom interactions in the many-body regime.

PACS numbers: 42.50.Ct, 42.70.Qs, 37.10.Gh

Interfacing light with atoms localized near nanophotonic structures has attracted increasing attention in recent years. Exemplary experimental platforms include nanofibers [1–3], photonic crystal cavities [4] and waveguides [5, 6]. Owing to their small optical loss and tight field confinement, these nanoscale dielectric devices are capable of mediating long-range atom-atom interactions using photons propagating in their guided modes. This new paradigm for strong interaction of atoms and optical photons offers new tools for scalable quantum networks [7], quantum phases of light and matter [8, 9], and quantum metrology [10].

In particular, powerful capabilities for dispersion and modal engineering in photonic crystal waveguides (PCWs) provide opportunities beyond conventional settings in AMO physics within the new field of *waveguide QED* [2, 3, 6, 11–13]. For example, the edge of a photonic band gap aligned near an atomic transition strongly enhances single-atom emission into the one-dimensional (1D) PCW due to a 'slow-light' effect [14–16]. Because the electric field of a guided mode near the band edge approaches a standing-wave, optical excitations can be induced in an array of trapped atoms with little propagation phase error, resulting in phase-matched superradiant emission [17, 18] into both forward and backward waveguide modes of the PCW. Superradiance has important applications for realizing quantum memories [19–23], single photon sources [24, 25], laser cooling by way of cooperative emission [26, 27], and narrow linewidth lasers [28]. Related cooperative effects are predicted in nano-photonic waveguides absent an external cavity [29], including atomic Bragg mirrors [30] and self-organizing crystals of atoms and light [31–33].

Complimentary to superradiant emission is the collective Lamb shift induced by proximal atoms virtually exchanging off-resonant photons [34–37]. With the atomic transition frequency placed in a photonic band gap of a PCW, real photon emission is largely suppressed. Coherent atom-atom interactions then emerge as a dominant effect for QED with atoms in bandgap materials [38–43]. Both the strength and length scale of the interaction can be 'engineered' by suitable band shaping of the PCW, as well as dynamically controlled by external lasers [42, 43]. Explorations of many-body physics with tunable and strong long-range atom-atom interactions are enabled [42, 43].

In this Letter, we present an experiment that cools, traps, and interfaces multiple atoms along a quasi one-dimensional PCW. Through precise band edge alignment and guided-mode (GM) design, we achieve strong radiative coupling of one trapped atom and a guided mode of the PCW, such that the inferred single-atom emission rate into the guided mode is $\Gamma_{\rm 1D}/\Gamma' = 1.0 \pm 0.1$, where $\Gamma_{\rm 1D}$ is the peak single-atom radiative decay rate into the guided mode and $\Gamma'$ is the radiative decay rate into all the other channels. With multiple atoms, we observe superradiant emission in both time and frequency domains. We infer superradiant coupling rate $\bar{\Gamma}_{\rm SR}$ that scales with the mean atom number $\bar{N}$ as $\bar{\Gamma}_{\rm SR} = \eta \bar{N} \cdot \Gamma_{\rm 1D}$ over the range $0.19 \lesssim \bar{N} \lesssim 2.6$ atoms, where $\eta = 0.34 \pm 0.06$.

We stress "waveguide" and not "cavity" QED because the dominant effects in our experiment are a result of the combination of atom-light localization within an area $A_{\rm w}$ comparable to the free-space atomic cross section, $A_{\rm w} \sim \lambda^2$, and an enhancement in the atom-field coupling due to band structure, namely a group index $n_g \approx 11$ that dominates over the enhancement $\mathcal{E}_I \sim 4$ from a weak external cavity with "mirror" reflectivity $R \approx 0.48$. By contrast, in conventional cavity QED, an atom interacts with a cavity mode with area $A_{\rm c} \gg \lambda^2$, $n_g \approx 1$, and an enhancement $\mathcal{E}_I \sim A_{\rm c}/\lambda^2 > 10^5$ (i.e., mirror reflectivity $R > 0.99999$) [22, 23].

Stated differently, in our PCW we are able to engineer the real and imaginary parts of the Green's function for atom-light interactions (e.g., Fig. SM3 in Ref. [45]) in ways that are not

[†] These authors contributed equally to this research.
[‡] Present address: Purdue University, West Lafayette, IN 47907, USA
[*] Correspondence and requests for materials should be addressed to HJK (hjkimble@caltech.edu.)

possible within the setting of conventional cavity QED. For example, our APCW enables many-body physics that is both non-trivial and inaccessible by using conventional optical cavities [42]. Our observation of superradiance demonstrates at least two important criteria toward the exploration of such new physics, namely (i) the capability to trap stably multiple atoms along a APCW, and therefore to build few-body quantum systems, extending to $N \sim 20$ atoms with improved trapping, and (ii) the ability to achieve relative band-edge alignment to better than $5\times10^{-4}$, which enables $n_g \gg 1$ with high-contrast Bloch modes.

Our experimental platform is based on trapped cesium atoms near a 1D alligator photonic crystal waveguide (APCW). The APCW consists of 150 identical unit cells with lattice constant $a = 371$nm and is terminated at either end by 30 tapered cells for mode matching to parallel nanobeams without corrugation. Design principles and device characterization can be found in Refs. [5, 6, 45]. For the APCW used here, we align the band edge of the TE-like fundamental guided mode near the cesium $D_1$ line at 894.6nm, with a mode-matched TE input field $E_{\rm in}$ tuned around the $6S_{1/2},\ F = 3 \rightarrow 6P_{1/2},\ F' = 4$ transition. Near the band edge, the atom-photon coupling rate is significantly enhanced by the group index $n_g \simeq 11$, and by reflections from the tapering regions, corresponding to an intensity enhancement $\mathcal{E}_I \sim 4$ [45].

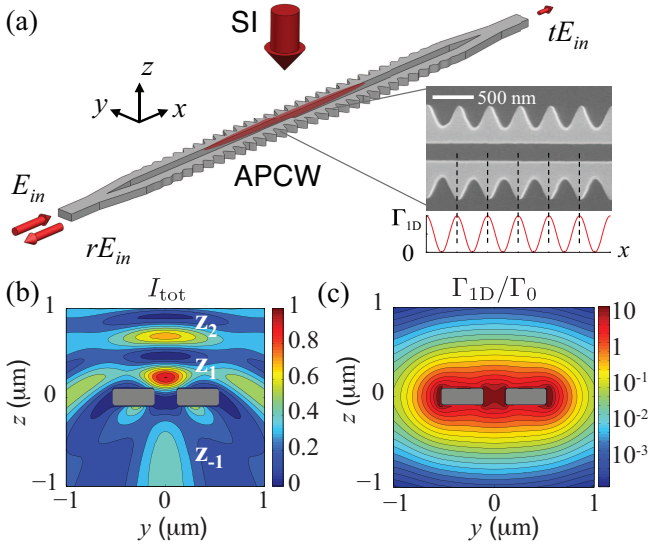


FIG. 1: Trapping and interfacing atoms with an APCW. (a) A side-illumination (SI) beam is reflected from an APCW (gray shaded structure) to form a dipole trap to localize atoms. The red shaded region represents trapped atoms along the APCW. An incident field $E_{\rm in}$ excites the TE-like mode and trapped atoms couple to this guided mode. The inset shows an SEM image of the APCW and corresponding single-atom coupling rate $\Gamma_{1D}$ along the $x$ axis at the center of the gap ($y = 0$). (b) Normalized intensity cross section of the total intensity $I_{\rm tot}$ resulting from the SI beam and its reflection. Trap locations along the $z$ axis at $y = 0$ are marked by $z_i$. Masked gray areas represent the APCW. (c) The single-atom coupling rate into the TE-like guided mode $\Gamma_{1D}(0, y, z)$ normalized to $\Gamma_0$ where $\Gamma_0$ is the Einstein-$A$ coefficient for free space.

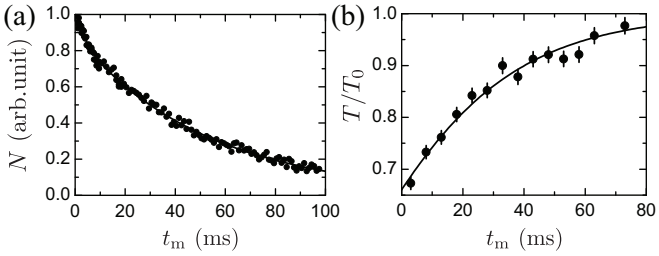


FIG. 2: Lifetime of trapped atoms near the APCW. (a) $1/e$-lifetime of $\tau_{\rm fs} = 54\pm5$ ms is determined using free-space absorption imaging of the trapped atom cloud. (b) $1/e$-lifetime of $\tau_{\rm GM} = 28 \pm 2$ ms is observed from the normalized transmission $T/T_0$ of resonant GM probe.

To trap atoms along the APCW, we create tight optical potentials using the interference pattern of a side-illumination (SI) beam and its reflection from the surface of the APCW [4]. The polarization of the SI beam is aligned parallel to the $x$-axis to maximize the reflected field. Figure 1(b) shows the calculated near-field intensity distribution in the $y$-$z$ plane [46]. With a red-detuned SI beam, cold atoms can be localized to intensity maxima (e.g., positions $z_{-1}, z_1, z_2$ in Fig.1(b)). However, because of the exponential falloff of the GM intensity, only those atoms sufficiently close to the APCW can interact strongly with guided-mode photons of the input field $E_{\rm in}$, shown in Fig.1(c). The trap site with the strongest atom-photon coupling is located at $(y_1, z_1) = (0, 220)$ nm, and $\Delta z \sim 120$ nm is the distance from the plane of the upper surfaces of the APCW. Other locations are calculated to have coupling to the guided mode less than 1% of that for site $z_1$.

Along the $x$ axis of the APCW, the dipole trap $U(x, 0, z_1)$ is insensitive to the dielectric corrugation within a unit cell and is nearly uniform within $< 2\%$ around the central region of the APCW. By contrast, atomic emission into the TE-like mode is strongly modulated with $\Gamma_{1D}(x, 0, z_1) \simeq \Gamma_{1D}\cos^2(kx)$ due to the standing-wave like coupling rate near the band edge ($k \approx \pi/a$), as shown in the inset of Fig.1(a). Thus, even for atoms uniformly distributed along the $x$ axis, only those close to the center of a unit cell can strongly couple to the guided mode. We choose a 50 $\mu$m waist for the SI beam to provide weak confinement along the $x$ axis, with atoms localized near the central region ($\Delta x \simeq \pm10$ $\mu$m) of the APCW for the estimated temperature $\sim 50\mu$K from a time-of-flight measurement in free space.

Cold atoms from a MOT that surrounds the APCW [6] are loaded into the dipole trap during an optical molasses phase ($\sim 5$ ms) and then optically pumped to $6S_{1/2},\ F = 3$ ($\sim 1$ ms). Atoms are held in the dipole trap for time $t_{\rm hold}$ relative to the end of the loading sequence, and then free-space absorption imaging is initiated over the interval $(t_{\rm hold}, t_{\rm hold} + \Delta t_{\rm m})$ with $\Delta t_{\rm m} = 0.2$ ms. We introduce the measured time $t_{\rm m} = t_{\rm hold} + \Delta t_{\rm m}/2$, centered in the measurement window. As shown in Fig.2(a), we measure a trap lifetime $\tau_{\rm fs} = 54 \pm 5$

ms and a peak density $\rho_0 \approx 2 \times 10^{11}$ cm$^{-3}$ near the APCW.

To determine the lifetime for trapped atoms along the APCW, we again hold atoms for $t_{\rm hold}$, and then launch $E_{\rm in}$ as a resonant GM probe with $\Delta t_{\rm m} = 5$ ms. From the transmitted signals, we compute $T/T_0$, where $T_0$ is the transmission without atoms. During the probe period, we also apply free-space repump beams, tuned to the $D_2$, $6S_{1/2}$, $F = 4 \rightarrow 6P_{3/2}$, $F' = 4$ resonance, to remove population in $6S_{1/2}$, $F = 4$, since the probe excites an open transition. Fig.2(b) shows $T/T_0$ gradually recovering to $T/T_0 = 1$ as $t_{\rm m}$ increases, with a fit to the data giving a $1/e$-time of $\tau_{\rm GM} = 28 \pm 2$ ms. Effects leading to $\tau_{\rm GM} < \tau_{\rm fs}$ are discussed in [45].

Our principal investigation of superradiance involves observation of the transient decay of both forward and backward emission from atoms trapped along the APCW. We excite superradiance by employing weak and short excitation pulses (FWHM 10ns) with an average photon number $N_{\rm p} \ll 1$ per pulse, ensuring a small degree of excitation can be uniformly shared among all ground state atoms. For a collection of $N > 1$ atoms, superradiance is heralded by a total decay rate $\Gamma_{\rm tot} = \Gamma_{\rm SR} + \Gamma^{(1)}_{\rm tot}$ that is enhanced beyond the total decay rate for one atom $\Gamma^{(1)}_{\rm tot} = \Gamma_{\rm 1D} + \Gamma'$. $\Gamma_{\rm SR}$ is the $N$-dependent superradiant rate operationally determined from $\Gamma_{\rm tot}$ and $\Gamma^{(1)}_{\rm tot}$. Here, $\Gamma'$ is the radiative decay rate into all channels other than the TE-like guided mode. We numerically evaluate $\Gamma'/\Gamma_0 \approx 1.1$ for an atom at the trap site $z_1$ in Fig.1(b) along the APCW where $\Gamma_0$ is the Einstein-$A$ coefficient for free space [15].

We record the temporal profiles of either forward or backward atomic emission into the guided mode following short-pulse ($\sim$10 ns FWHM), resonant excitations via $E_{\rm in}$. After a time $t_{\rm hold}$ the excitation cycle is repeated every 500 ns for $\Delta t_{\rm m} = 6$ ms, and detection events are accumulated for the reflected intensity. We consider decay curves of GM emission at 15 ns $< t_{\rm e} <$ 70 ns after the center of the excitation pulse [45]. The total decay rate $\bar{\Gamma}_{\rm tot}$ is extracted by exponential fits as shown in the inset of Fig.3(a).

Enhanced total decay rate with increasing atom number is evidenced in Fig.3(a), where the atom number is adjusted by varying trap hold time $t_{\rm hold}$ prior to the measurement. At the shortest measurement time $t_{\rm m} = 3$ ms with $t_{\rm hold} = 0$ ms, the measured total decay rate is largest at $\bar{\Gamma}_{\rm tot}/\Gamma_0 \approx 2.9$. At $t_{\rm m} = 63$ ms, much longer than the trap lifetime $\tau_{\rm GM} = 28 \pm 2$ ms, the total decay rate settles to $\bar{\Gamma}_{\rm tot}/\Gamma_0 \approx 2.0$. This asymptotic behavior suggests that $\bar{\Gamma}_{\rm tot}$ at long hold time corresponds to the single-atom decay rate $\bar{\Gamma}^{(1)}_{\rm tot}$.

To determine quantitatively the superradiant and single-atom emission rates, we present two different analyses that yield consistent results. First is a simple and intuitive analysis applied to Fig.3(a) in which we employ an empirical exponential fit, $\bar{\Gamma}_{\rm tot}(t_{\rm m}) = \bar{\Gamma}_{\rm SR} e^{-t_{\rm m}/\tau_{\rm SR}} + \bar{\Gamma}^{(1)}_{\rm tot}$, with the maximum superradiant $\bar{\Gamma}_{\rm SR}$, single-atom $\bar{\Gamma}^{(1)}_{\rm tot}$, and $\tau_{\rm SR}$ characterizing decay of superradiance due to the atom loss. The fit yields $\bar{\Gamma}_{\rm SR}/\Gamma_0 = 1.1 \pm 0.1$ with $\tau_{\rm SR} = 17 \pm 3$ ms, as shown by the red curve in Fig.3(a). The asymptote $\bar{\Gamma}^{(1)}_{\rm tot}/\Gamma_0 = 2.0 \pm 0.1$ gives the total single-atom decay rate. With $\Gamma'/\Gamma_0 \approx 1.1$, we deduce $\bar{\Gamma}_{\rm 1D}/\Gamma_0 = 0.9 \pm 0.1$.

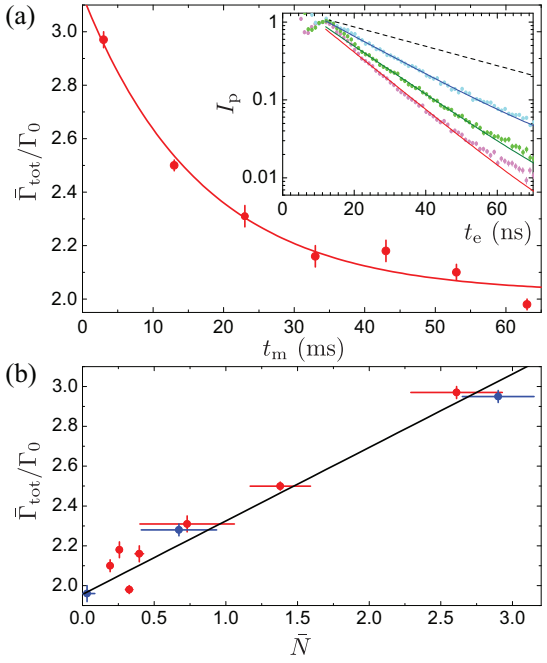


FIG. 3: Decay rate and atom number. (a) Fitted total decay rate $\bar{\Gamma}_{\rm tot}$ normalized with $\Gamma_0$ (circles) as a function of measurement time $t_{\rm m}$. The solid line is an exponential fit to determine the superradiant decay rate $\bar{\Gamma}_{\rm SR}/\Gamma_0 = 1.1 \pm 0.1$ and the single-atom decay rate $\bar{\Gamma}^{(1)}_{\rm tot}/\Gamma_0 = 2.0 \pm 0.1$ with $\tau_{\rm SR} = 17 \pm 3$ ms. The inset shows the normalized temporal profiles of backward emission $I_{\rm p}$. Exponential fits (solid curves): $t_{\rm m} = 3$ ms (red), 13 ms (green), and 63 ms (blue). The black dashed curve shows exponential decay with $\Gamma_0$. (b) Fitted total decay rate $\bar{\Gamma}_{\rm tot}/\Gamma_0$ as a function of mean number of trapped atoms $\bar{N}$. We adjust $\bar{N}$ by changing the trap hold time (red) or atom loading time (blue). The black line is a linear fit to the combined data sets, giving $\bar{\Gamma}_{\rm SR} = \eta \cdot \bar{N} \cdot \Gamma_{\rm 1D}$ with $\eta = 0.34 \pm 0.06$.

To substantiate this empirical model, our second analysis is a detailed numerical treatment based upon transfer matrix calculations [45]. Decay curves are generated for a fixed number of atoms $N$ distributed randomly along the $x$-axis of the APCW with spatially-varying coupling $\Gamma_{\rm 1D}(x) \simeq \Gamma_{\rm 1D} \cos^2(kx)$. These $N$-dependent, spatially-averaged decay curves are further averaged over a Poisson distribution with mean atom number $\bar{N}$. Fitting to this model, we extract $\Gamma_{\rm 1D}/\Gamma_0 = 1.1 \pm 0.1$ for measurements at long hold time $t_{\rm m} = 63$ ms in Fig.3(a). Since the GM emission is spatially modulated by $\cos^4(kx)$, only an atom near the center of unit cell can strongly couple to the guided mode, resulting in the small difference between averaged $\bar{\Gamma}_{\rm 1D}$ and peak $\Gamma_{\rm 1D}$. Also, the decay curve for GM emission at $t_{\rm m} = 3$ ms is well fitted with $\bar{N} = 2.6 \pm 0.3$ atoms [45]. The red points in Fig.3 (b) display the total decay rate $\bar{\Gamma}_{\rm tot}$ as a function of $\bar{N}$ extracted from the model fits, which shows that superradiance emission rate is proportional to $\bar{N}$.

$\Gamma_{\rm 1D}/\Gamma' = 1.0 \pm 0.1$ from our measurements agrees reason-

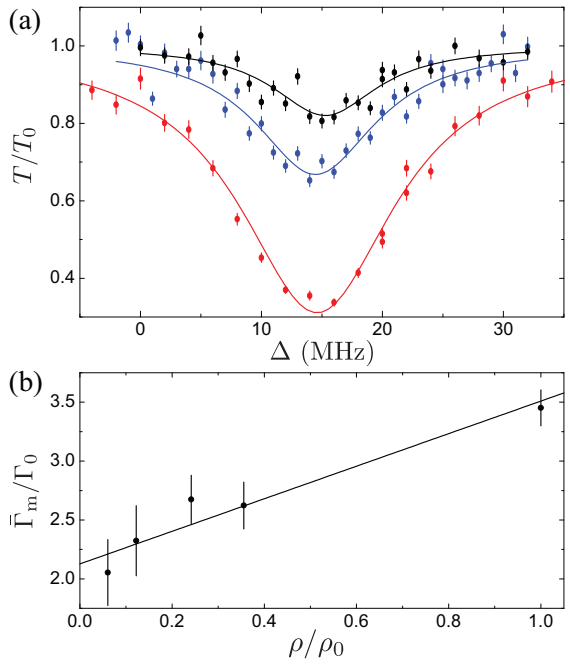


FIG. 4: Steady-state transmission spectra $T(\Delta)$ and fitted atomic linewidth $\bar{\Gamma}_{\rm m}$. (a) $T(\Delta)$ with $\Delta = 0$ corresponding to the free-space line center. The three sets of points are measured at relative densities $\rho/\rho_0 = 0.12$ (black), 0.24 (blue), and 1 (red). Solid curves are Lorentzian fits to determine the linewidth $\bar{\Gamma}_{\rm m}$. (b) Fitted linewidths (circles) normalized to $\Gamma_0$ as a function of $\rho/\rho_0$. The solid line is a linear fit with intercept of $\bar{\Gamma}_{\rm m}^{(1)}/\Gamma_0 = 2.1 \pm 0.1$.

ably well with the theoretical value $\Gamma_{\rm 1D}/\Gamma' \approx 1.1$ determined by FDTD calculations [44, 45], despite several uncertainties (e.g., locations of trap minima). The agreement validates the precision of our fabricated samples as well as the power of the theoretical tools [15, 42, 43].

We confirm that the variation of $\bar{\Gamma}_{\rm tot}$ in Fig.3(a) is not due to the heating of atomic motion during the trap hold time. To see this, we adjust $\bar{N}$ via different MOT loading times and measure the decay rate at the shortest hold time ($t_{\rm m} = 3$ ms), as shown by blue points in Fig.3(b). These observations are consistent with those from varying the trap hold time (red points in Fig.3(b)), and lead to an almost identical single-atom decay rate $\bar{\Gamma}_{\rm tot}^{(1)}/\Gamma_0 = 2.0 \pm 0.1$ at the shortest loading time, corresponding to $\rho/\rho_0 = 0.16$ and $\bar{N} \ll 1$.

The data and our analysis related to Fig.3 strongly support the observation of superradiance for atoms trapped along the APCW. Assuming $\bar{\Gamma}_{\rm tot} = \bar{\Gamma}_{\rm SR} + \bar{\Gamma}_{\rm tot}^{(1)}$ and fitting $\bar{\Gamma}_{\rm tot}$ linearly with $\bar{N}$, as shown in Fig.3(b), we find that the superradiant rate is given by $\bar{\Gamma}_{\rm SR} = \eta \cdot \bar{N} \cdot \Gamma_{\rm 1D}$ with $\eta = 0.34 \pm 0.06$. For a motivation of the scaling of the superradiant coupling rate and a physical interpretation of the constant $\eta$, see [45].

This observation of superradiance is complemented by line broadening for steady-state transmission spectra $T(\Delta)$ measured at $t_{\rm m} = 3$ ms with $\Delta t_{\rm m} = 5$ ms in Fig.4. The measured linewidths $\bar{\Gamma}_{\rm m}$ are significantly broader than the free-space width $\Gamma_0/2\pi = 4.56$ MHz [47]. We also measure $T/T_0 \simeq 0.30$ at line center for maximum density $\rho_0$, due to strong atom-photon coupling.

No clear density dependent shift is observed in Fig.4(a), in support of our neglect of cooperative energy shifts $|H_{\rm dd}|$ [45]. The shift in line center for $T(\Delta)$ from $\Delta = 0$ in free space to $\Delta = 14$ MHz for trapped atoms is induced by the dipole trap. Furthermore, trapped atoms should suffer small inhomogeneous broadening in the spectra, since the light shift induced by the dipole trap is small ($< 1$ MHz) for the $6P_{1/2}, F = 4'$ excited state, and atoms are well localized around the trap center due to their low temperature $T \sim 50\mu$K, corresponding to a small range of light shifts $\lesssim 1$MHz for the ground state.

In Fig.4 (b), we plot the linewidths $\bar{\Gamma}_{\rm m}$ extracted from $T(\Delta)$ as a function of $\rho/\rho_0$. $\bar{\Gamma}_{\rm m}/\Gamma_0 \approx 3.4$ is largest at $\rho/\rho_0 = 1$, and reduces to $\bar{\Gamma}_{\rm m}/\Gamma_0 \approx 2.1$ at $\rho/\rho_0 = 0.06$. From linear extrapolation, the single-atom linewidth is estimated to be $\bar{\Gamma}_{\rm m}^{(1)}/\Gamma_0 = 2.1 \pm 0.1$. Absent inhomogeneous broadening, we expect $\bar{\Gamma}_{\rm m}^{(1)} = \bar{\Gamma}_{\rm 1D} + \Gamma'$. With $\Gamma'/\Gamma_0 \approx 1.1$, the single-atom coupling rate is deduced as $\bar{\Gamma}_{\rm 1D}/\Gamma_0 \approx 1.0 \pm 0.1$. A simple estimate of the maximum mean number of atoms follows from $\bar{N}_{\rm m} = (\bar{\Gamma}_{\rm m}(\rho_0) - \Gamma')/\bar{\Gamma}_{\rm 1D} \simeq 2.4 \pm 0.4$ atoms [48].

In conclusion, we have demonstrated superradiance for atoms trapped along the APCW and a peak single-atom coupling rate $\Gamma_{\rm 1D}/\Gamma' = 1$ inferred, where $\Gamma'/\Gamma_0 \approx 1.1$ is the radiative decay rate into all the other channels. Our weak trap along the APCW is a promising platform to study optomechanical behavior induced by the interplay between sizable single-atom reflectivity and large optical forces, and investigations of spin-motion coupling [32, 33]. By optimizing the power and detuning of an auxiliary GM field, it should be possible to transport these trapped atoms into trap sites centered within the vacuum gap [15], and achieve stable trapping and ground-state cooling [49, 50]. We expect $\Gamma_{\rm 1D}$ to increase by more than five-fold [15]. Opportunities for new physics in the APCW arise by fabricating devices with the atomic resonance inside the band gap to induce long-range atom-atom interactions [41–43], enabling investigations of novel quantum transport and many-body phenomena.

*Acknowledgements* We gratefully acknowledge the contributions of D. J. Alton, D. E. Chang, K. S. Choi, J. D. Cohen, J. H. Lee, M. Lu, M. J. Martin, A. C. McClung, S. M. Meenehan, L. Peng, and R. Norte. Funding is provided by the IQIM, an NSF Physics Frontiers Center with support of the Moore Foundation, and by the DoD NSSEFF program (HJK), the AFOSR QuMPASS MURI, NSF PHY-1205729 (HJK) and the DARPA ORCHID program. AG is supported by the Nakajima Foundation. SPY and JAM acknowledge support from the International Fulbright Science and Technology Award.

[1] D. E. Chang, V. Vuletić, and M. D. Lukin, *Nat. Photon.* **8**, 685 (2014).
[2] E. Vetsch, D. Reitz, G. Sagué, R. Schmidt, S. T. Dawkins, and A. Rauschenbeutel, *Phys. Rev. Lett.* **104**, 203603 (2010).

[3] A. Goban, K. S. Choi, D. J. Alton, D. Ding, C. Lacroute, M. Pototschnig, T. Thiele, N. P. Stern, and H. J. Kimble, *Phys. Rev. Lett.* **109**, 033603 (2012).

[4] J. D. Thompson, T. G. Tiecke, N. P. de Leon, J. Feist, A. V. Akimov, M. Gullans, A. S. Zibrov, V. Vuletić, and M. D. Lukin, *Science* **340**, 1202 (2013).

[5] S.-P. Yu, J. D. Hood, J. A. Muniz, M. J. Martin, R. Norte, C.-L. Hung, S. M. Meenehan, J. D. Cohen, O. Painter, and H. J. Kimble, Appl. Phys. Lett. **104**, 111103 (2014).

[6] A. Goban, C. -L. Hung, S. -P. Yu, J. D. Hood, J. A. Muniz, J. H. Lee, M. J. Martin, A. C. McClung, K. S. Choi, D. E. Chang, O. Painter, and H. J. Kimble, *Nat. Commun.* **5**, 3808 (2014).

[7] H. J. Kimble, *Nature* **453**, 1023-1030 (2008).

[8] M. J. Hartmann, F. G. S. L. Brandao, and M. B. Plenio, *Nat. Phys.* **2**, 462 (2006).

[9] A. D. Greentree, C. Tahan, J. H. Cole, and L. C. L. Hollenberg, *Nat. Phys.* **2**, 856 (2006).

[10] P. Kómár, E. M. Kessler, M. Bishof, L. Jiang, A. S. Sørensen, J. Ye and M. D. Lukin, *Nat. Phys* **10**, 582-587 (2014).

[11] D. E. Chang, A. S. Sørensen, E. A. Demler, and M. D. Lukin, *Nat. Phys.* **3**, 807-812 (2007).

[12] A. L. van Loo, A. Fedorov, K. Lalumière, B. C. Sanders, A Blais, and A. Wallraff, *Science* **342** 1494 (2013).

[13] J. A. Mlynek, A. A. Abdumalikov, C. Eichler, and A. Wallraff, *Nat. Commun.* **5**, 5186 (2014).

[14] T. Baba, *Nat. Photon.* **2**, 465-473 (2008).

[15] C.-L. Hung, S. M. Meenehan, D. E. Chang, O. Painter and H. J. Kimble, *New J. Phys.* **15**, 083026 (2013).

[16] P. Lodahl, S. Mahmoodian, amd S. Stobbe, *Rev. Mod. Phys.* (2015); *arXiv*:1312.1079.

[17] R. H. Dicke, *Phys. Rev.* **93**, 99-110 (1954).

[18] M. Gross and S. Haroche, *Phys. Rep.* **93**, 301 (1982).

[19] L.-M. Duan, M. D. Lukin, J. I. Cirac, and P. Zoller, *Nature* **414**, 413 (2001).

[20] C. H. van der Wal, M. D. Eisaman, A. André, R. L. Walsworth, D. F. Phillips, A. S. Zibrov and M. D. Lukin, *Science* **301** 196-200 (2003).

[21] A. Kuzmich, W. P. Bowen, A. D. Boozer, A. Boca, C. W. Chou, L.-M. Duan and H. J. Kimble, *Nature* **423**, 731-734 (2003).

[22] B. Casabone, K. Friebe, B. Brandstätter, K. Schüppert, R. Blatt, and T. E. Northup, *Phys. Rev. Lett.* **114** 023602 (2015).

[23] R. Reimann, W. Alt, T. Kampschulte, T. Macha, L. Ratschbacher, N. Thau, S. Yoon, and D. Meschede, *Phys. Rev. Lett.* **114** 023601 (2015).

[24] C. W. Chou, S. V. Polyakov, A. Kuzmich and H. J. Kimble, *Phys. Rev. Lett.* **92** 213601 (2004).

[25] A. T. Black, J. K. Thompson and V. Vuletic, *Phys. Rev. Lett.* **95**, 133601 (2005).

[26] H. W. Chan, A. T. Black, and V. Vuletic, *Phys. Rev. Lett.* **90**, 063003 (2003).

[27] M. Wolke, J. Klinner, H. Keßler, and A. Hemmerich, *Science* **337**, 75 (2012).

[28] J. G. Bohnet, Z. Chen, J. M. Weiner, D. Meiser, M. J. Holland, and J. K. Thompson, *Nature* **484**, 78 (2012).

[29] F. Le Kien, S. D. Gupta, K. P. Nayak, and K. Hakuta, *Phys Rev A* **72**, 063815 (2005).

[30] D. E. Chang, L. Jiang, A. V. Gorshkov and H. J. Kimble, *New J. Phys.* **14** 063003 (2012).

[31] I. H. Deutsch, R. J. C. Spreeuw, S. L. Rolston and W. D. Phillips, *Phys. Rev. A* **52**, 1394 (1995).

[32] D. E. Chang, J. I. Cirac, and H. J. Kimble, *Phys. Rev. Lett.* **110**, 113606 (2013).

[33] T. Grießer, and H. Ritsch, *Phys. Rev. Lett.* **111**, 055702 (2013).

[34] A. Svidzinsky and J. -T. Chang, *Phys. Rev. A* **77**, 043833 (2008).

[35] M. O. Scully, *Phys. Rev. Lett.* **102**, 143601 (2009).

[36] R. Röhlsberger, K. Schlage, B. Sahoo, S. Couet, and R. Rffer, *Science* **328** 5983 (2010).

[37] J. Keaveney, A. Sargsyan, U. Krohn, I. G. Hughes, D. Sarkisyan and C. S. Adams *Phys. Rev. Lett.*, **108** 173601 (2012).

[38] S. John and J. Wang, *Phys. Rev. Lett.* **64** 2418 (1990).

[39] G. Kurizki, *Phys. Rev. A* **42**, 2915 (1990).

[40] P. Lambropoulos, G. M. Nikolopoulos, T. R. Nielsen, and S. Bay, *Rep. Prog. Phys.* **63**, 455 (2000).

[41] E. Shahmoon and G. Kurizki, *Phys. Rev. A* **87**, 033831 (2013).

[42] J. S. Douglas, H. Habibian, C. -L. Hung, A. V. Gorshkov, H. J. Kimble and D. E. Chang, *Nat. Photon.* **9**, 326-331 (2015).

[43] A. Gonzlez-Tudela, C.-L. Hung, D. E. Chang, J. I. Cirac and H. J. Kimble, *Nat. Photon.* **9**, 320-325 (2015).

[44] A. F. Oskooi, D. Roundy, M. Ibanescu, P. Bermel, J. D. Joannopoulos, and S. G. Johnson, *Comp. Phys. Comm*, **181**, 687-702 (2010).

[45] See accompanying Supplemental Material for detailed discussion of ACPW, lifetime measurements, and decay rate analyses, which includes Refs. [5, 11, 15, 30, 31, 51–55].

[46] COMSOL, http://www.comsol.com.

[47] R. J. Rafac, C. E. Tanner, A. E. Livingston, and H. G. Berry, *Phys. Rev. A* **60**, 3648 (1999).

[48] $\bar{N}_{\rm m}$ is defined from $\bar{\Gamma}_{\rm m}(\rho) = \bar{N}_{\rm m}\bar{\Gamma}_{\rm 1D} + \Gamma'$ for an approximate estimate of the number of atoms. Empirically we find $\bar{N}_{\rm m} \sim \bar{N}$.

[49] J. D. Thompson, T. G. Tiecke, A. S. Zibrov, V. Vuletić, and M. D. Lukin, *Phys. Rev. Lett.* **110**, 133001 (2013).

[50] A. M. Kaufman, B. J. Lester, and C. A. Regal, *Phys. Rev. X* **2**, 041014 (2012).

[51] J. D. Hood *et al. in preparation* (2015).

[52] G. S. Agarwal, *Phys. Rev. A* **12** 1475 (1975).

[53] S. Y. Buhmann, L. Knöll, D.-G. Welsch and H. T. Dung, *Phys. Rev. A* **70**, 052117 (2004).

[54] S. Y. Buhmann and D.-G. Welsch, *Phys. Rev. A* **77**, 012110 (2008).

[55] R. J. Thompson, Q. A. Turchette, O. Carnal, and H. J. Kimble, *Phys. Rev. A* **57**, 3084 (1998).